Mosaic Activating Mutations in GNA11 and GNAQ Are Associated with Phakomatosis Pigmentovascularis and Extensive Dermal Melanocytosis

Accepted Manuscript

Mosaic activating mutations in *GNA11* and *GNAQ* are associated with Phakomatosis Pigmentovascularis and Extensive Dermal Melanocytosis

Anna C. Thomas, Zhiqiang Zeng, Jean-Baptiste Rivière, Ryan O'Shaughnessy, Lara Al-Olabi, Judith St-Onge, David J. Atherton, Hélène Aubert, Lorea Bagazgoitia, Sébastien Barbarot, Emmanuelle Bourrat, Christine Chiaverini, W Kling Chong, Yannis Duffourd, Mary Glover, Leopold Groesser, Smail Hadj-Rabia, Henning Hamm, Rudolf Happle, Imran Mushtaq, Jean-Philippe Lacour, Regula Waelchli, Marion Wobser, Pierre Vabres, E. Elizabeth Patton, Veronica A. Kinsler

PII: S0022-202X(16)00332-8

DOI: 10.1016/j.jid.2015.11.027

Reference: JID 128

To appear in: *The Journal of Investigative Dermatology*

Received Date: 29 June 2015

Revised Date: 31 October 2015

Accepted Date: 2 November 2015

Please cite this article as: Thomas AC, Zeng Z, Rivière J-B, O'Shaughnessy R, Al-Olabi L, St-Onge J, Atherton DJ, Aubert H, Bagazgoitia L, Barbarot S, Bourrat E, Chiaverini C, Chong WK, Duffourd Y, Glover M, Groesser L, Hadj-Rabia S, Hamm H, Happle R, Mushtaq I, Lacour J-P, Waelchli R, Wobser M, Vabres P, Patton EE, Kinsler VA, Mosaic activating mutations in *GNA11* and *GNAQ* are associated with Phakomatosis Pigmentovascularis and Extensive Dermal Melanocytosis, *The Journal of Investigative Dermatology* (2016), doi: 10.1016/j.jid.2015.11.027.

Title

Mosaic activating mutations in *GNA11* and *GNAQ* are associated with Phakomatosis Pigmentovascularis and Extensive Dermal Melanocytosis

Authors

Anna C. Thomas[1*], Zhiqiang Zeng[2*], Jean-Baptiste Rivière[3*], Ryan O'Shaughnessy[4], Lara Al-Olabi[1], Judith St-Onge[3], David J. Atherton[5], Hélène Aubert[6], Lorea Bagazgoitia[7], Sébastien Barbarot[6], Emmanuelle Bourrat[8,9], Christine Chiaverini[10], W Kling Chong[11], Yannis Duffourd[3], Mary Glover[5], Leopold Groesser[12], Smail Hadj-Rabia[13], Henning Hamm[14], Rudolf Happle[15], Imran Mushtaq[16], Jean-Philippe Lacour[10], Regula Waelchli[5], Marion Wobser[14], Pierre Vabres[3,17§], E. Elizabeth Patton[2§] and Veronica A. Kinsler[1,5§]

Affiliations

1. Genetics and Genomic Medicine, UCL Institute of Child Health, London, UK
2. MRC Institute of Genetics and Molecular Medicine, MRC Human Genetics Unit & Edinburgh Cancer Research UK Centre, Edinburgh, UK
3. Equipe d'Accueil 4271, Génétique des Anomalies du Développement, University of Burgundy, Dijon, France
4. Livingstone Skin Research Unit, UCL Institute of Child Health, London, UK
5. Paediatric Dermatology, Great Ormond Street Hospital for Children, London, UK
6. Department of Dermatology, Nantes University Hospital, Nantes, France.
7. Dermatology, Hospital Universitario Ramón y Cajal, Madrid, Spain
8. Dermatology, Saint-Louis Hospital, Paris, France
9. General Paediatrics, Robert-Debré Hospital, Paris, France

10. Dermatology, University Hospital of Nice, Nice, France
11. Neuroradiology, Great Ormond St Hospital for Children, London, UK
12. Dermatology, Regensburg University Clinic, Regensburg, Germany
13. Paediatric Dermatology, Necker Enfants-Malades Hospital, Paris, France
14. Dermatology, University Hospital Wuerzburg, Wuerzburg, Germany
15. Dermatology, Freiburg University Medical Center, University of Freiburg, Germany
16. Paediatric Urology, Great Ormond Street Hospital for Children, London, UK
17. Dermatology, Dijon University Hospital, Dijon, France

*These authors contributed equally to this work

[§] These authors contributed equally to this work

Corresponding authors

Veronica Kinsler, Genetics and Genomic Medicine, UCL Institute of Child Health, 30 Guilford Street, London WC1N 1EH, UK.

Phone: +44 (0)207 242 9789.

Email: v.kinsler@ucl.ac.uk

Elizabeth Patton, MRC Institute of Genetics and Molecular Medicine, MRC Human Genetics Unit & Edinburgh Cancer Research UK Centre, Edinburgh, UK

Phone: +44 (0)131 651 8500

Email: e.patton@igmm.ed.ac.uk

Location of work

The laboratory work was carried out in London, UK, Edinburgh, UK, and Dijon, France

Short title

GNA11 and *GNAQ* mosaicism

Abbreviations

PPV – phakomatosis pigmentovascularis

Abstract

Common birthmarks can be an indicator of underlying genetic disease, but are often overlooked. Mongolian Blue Spots (dermal melanocytosis) are usually localized and transient, but can be extensive, permanent and associated with extra-cutaneous abnormalities. Co-occurrence with vascular birthmarks defines a subtype of Phakomatosis Pigmentovascularis (PPV), a group of syndromes associated with neuro-vascular, ophthalmological, overgrowth and malignant complications. Here, we discover that extensive dermal melanocytosis and PPV are associated with activating mutations in *GNA11* and *GNAQ*, genes that encode Gα subunits of heterotrimeric G-proteins. The mutations were detected at very low level in affected tissues but were undetectable in the blood, indicating that these conditions are post-zygotic mosaic disorders. *In vitro* expression of mutant $GNA11^{R183C}$ and $GNA11^{Q209L}$ in human cell lines demonstrated activation of the downstream p38 MAPK signalling pathway, and the p38, JNK and ERK pathways respectively. Transgenic mosaic zebrafish models expressing mutant $GNA11^{R183C}$ under promoter *mitfa* developed extensive dermal melanocytosis recapitulating the human phenotype. PPV and extensive dermal melanocytosis are therefore diagnoses in the group of mosaic heterotrimeric G-protein disorders, joining McCune-Albright and Sturge-Weber syndromes. These findings will allow accurate clinical and molecular diagnosis of this subset of common birthmarks, thereby identifying infants at risk of serious complications, and will provide novel therapeutic opportunities.

Introduction

Mongolian Blue Spots (or more appropriately dermal melanocytosis) are very common birthmarks, seen in up to 95% of African neonates, and approximately 10% of white Caucasians (1). As a result they are easily overlooked as a possible sign of underlying genetic disease. Classically they are flat, dark-blue lesions with indistinct edges overlying the buttocks and lower back, which undergo spontaneous resolution over a period of years. However, the appearances and behavior are not always classical (2), with some dermal melanocytosis involving unusual sites, covering large areas of the body surface, being more deeply pigmented and better-defined, and persisting rather than resolving. These more atypical patterns of dermal melanocytosis can be associated with anomalies such as co-localised cleft lip (3), ocular melanocytosis (4), ocular melanoma (5), lysosomal storage disorders (6), or vascular birthmarks. This latter association then falls under the diagnostic group of Phakomatosis pigmentovascularis (PPV) (for clinical examples see Figure 1). PPV is a group of sporadic disorders of unknown frequency, defined by the co-occurrence of pigmentary and vascular birthmarks, and sub-classified clinically by the exact cutaneous phenotypes (supplementary table 1)(7-9). It has not been clear if the subtypes are distinct disorders or variable expressions of a single disorder, as the molecular and developmental pathogenesis of PPV has been unknown. The hypothesis of 'non-allelic twin-spotting' was previously expounded to explain the co-occurrence of two disparate birthmarks (10), however this has recently been retracted by the author due to lack of supporting molecular evidence (11). Extra-cutaneous associations of PPV can be severe, including scleral or intraocular melanocytosis (12), glaucoma (13-15), intracerebral vascular or other malformations leading to seizures and cognitive delay (12, 16-18), overgrowth of soft tissues or limbs (18-20), and melanoma. The latter can arise in choroid or conjunctiva, with

melanocytoma of the optic disc also described (12, 13, 21, 22). Without an understanding of the genetic pathogenesis of the disease targeted therapies for the congenital and neoplastic aspects of the disease have been impossible.

When considering the genetic basis of extensive dermal melanocytosis and of PPV, we hypothesized that these conditions could be the result of a post-zygotic mutation in a member of the G-protein nucleotide binding protein alpha subunit family. This hypothesis was generated by the rare concurrent description of PPV with Sturge-Weber syndrome (SWS)(15, 19), a vascular disorder with no pigmentary phenotype, recently found to be due to post-zygotic mosaicism for activating muatations in *GNAQ* (23). We also hypothesized that the same mutation could be present in both types of birthmarks in PPV secondary to a single mutation in a pluripotent progenitor cell.

Results

Missense *GNA11* or *GNAQ* mutations were found in 8/11 patients tested. In each case these mutations were detected in affected skin (and in one case ocular tissue) at very low levels, and were undetectable in blood, indicating post-zygotic mosaicism (Table 1). Where levels of mutant allele of <1% were detected in blood these were not able to be distinguished from background noise, despite the great depth of coverage (supplementary table 3), and are therefore called as wild-type. In the three patients with extensive dermal melanocytosis we identified mutations in *GNAQ* in two, one c.548G>A, p.R183Q, and one c.626A>C, Q209P. In the eight patients with PPV we identified somatic *GNA11* mutations in four - three at position c.547C>T, p.R183C, and one novel mutation in the same codon c.547C>A, p.R183S - and *GNAQ* mutations in two, both at position c.548G>A, p.R183Q (Fig. 2). Importantly there was conservation of mutation between pigmentary and vascular lesions in each patient where more than one skin biopsy was available (table 1 and supplementary table 3). Measured percentage of mosaicism in skin samples was at lowest 1.5%, using next generation sequencing mutant allele count as a percentage of the total number of reads (supplementary table 3). None of these mutations in *GNA11* and *GNAQ* are described in the largest current population database (24).

In *in vitro* transfection experiments HEK293 cells were transfected with vector, wild type *GNA11* or mutant *GNA11* constructs encoding R183C and Q209L. Figure 3 shows results of Western blots for Flag, total GNA11 and the phosphorylated and total p38, JNK, ERK and AKT in total protein lysates from these cells. Analysis of the ratio of phosphorylated to total p38, JNK, ERK and AKT normalized by the actin loading control (from two replicates, pooled results of WT compared to those of mutant) demonstrated increased phosphorylation

and therefore activation of the p38 MAPK pathway by the R183C mutant, and of ERK, p38 MAPK and JNK pathways by Q209L, in keeping with previous results for Q209L (25). These results were significant at 0.05 level using a one-tailed t-test.

GNA11^{R183C}- and *GNA11*^{Q209L}-expressing zebrafish exhibited dark cutaneous patches of melanocytes by one month. When the mutant transgenic zebrafish reached adulthood at 3 months, nearly all injected fish (n=17/18 for R183C and n=16/16 for Q209L) developed large and clearly visible pigmentary lesions (Fig. 4a,b), recapitulating the human phenotype of dermal melanocytosis. Wild type *GNA11* expression in melanocytes also produced mosaic animals with some pigmentary lesions (n=10/27), however these were usually smaller and less dark, suggesting that the melanocyte lineage is highly sensitive to GNA11-coupled receptor signaling. Histopathology revealed many extra melanocytes in both the epidermis (over the scales, not shown) and the dermis in the pigmentary lesion of mutant *GNA11*^{R183C} injected fish, with occasional involvement of the underlying muscle (Fig. 4c).

Discussion

We have sought to differentiate a subgroup of the common birthmark dermal melanocytosis where infants are at risk of extracutaneous complications, by elucidating the underlying genetic cause. We show here that extensive dermal melanocytosis and PPV are genetic conditions associated with post-zygotic mutations in genes encoding Gα subunits of heterotrimeric G proteins. Specifically, post-zygotic mutations in *GNAQ* have been found in extensive dermal melanocytosis, and mutations in *GNA11* or *GNAQ* have been found in PPV types I, II (cesioflammea), IV and V (cesiomarmorata), as well as the unclassifiable achromico-melano-marmorata type. Type IV is considered to be exceptionally rare and was not tested as no samples were available. Type III (spilorosea) is distinguished clinically from all other types of PPV by the absence of dermal melanocytosis, and as only one patient from this group was tested (and was wild-type) we cannot yet conclude anything about the genetic aetiology of this type. Of note the percentage mosaicism was often very low, the result of very few mutant cells within a skin biopsy of a completely macular birthmark, emphasizing the need for adequately sensitive detection techniques in this type of genetic disease. A possible alternative explanation for our findings is that these patients are somehow genetically predisposed to somatic mutations in the same genes, and this is particularly relevant for those in whom we have only been able to obtain one sample. Although this explanation cannot be entirely excluded it is much less convincing than post-zygotic mosaisicm, as we have found different mutations in different patients, and the same mutation present in more than location where two samples were obtained from one individual. As candidate gene sequencing was performed in this study we cannot exclude the presence of further mutation in other genes. Further exome sequencing could be done to look for secondary mutations.

True embryonic mosaicism has not hitherto been described for *GNA11* mutations. Isolated somatic *GNA11* mutations have been found in uveal melanoma and single blue naevi (26) (a lesion distinct from dermal melanocytosis both clinically and histologically), and in contrast to our findings in PPV the prevalence of codon 183 mutations in the single melanomas and blue naevi was very much lower than in codon 209 (26). Post-zygotic mosaicism for *GNAQ* mutations has been described as the major cause of Sturge-Weber syndrome (SWS), a purely vascular disorder with no pigmentary phenotype. Somatic mutations in *GNAQ* are frequent in uveal melanoma and single blue naevi(27). Our findings therefore not only describe *GNA11* mosaicism, but also extend the phenotype of human *GNAQ* mosaicism from SWS (vascular only), through to PPV (vascular and pigmentary), to extensive dermal melanocytosis (pigmentary only). Exactly how the same mutation can generate these three distinct phenotypes is not yet clear.

Codon 183 in both *GNA11* and *GNAQ* is located within the GTP binding region of the human G-alpha subunit, a region required for hydrolysis of GTP to GDP and an essential step for inactivation of G-protein coupled receptor signaling. These mutations therefore lead to a decrease in function of the GTPase, and to constitutive activation of downstream effector pathways. We have shown that the commonest mutation at codon 183 of *GNA11* activates the downstream p38 MAPK pathway in human cells, whereas the codon 209 mutant (not found in this cohort in *GNA11*, but in one patient in *GNAQ*) activates p38 MAPK, JNK and ERK pathways, broadly supporting previous findings of effects of mutations in both *GNA11* (25, 26) and *GNAQ* (26).

Interestingly different mutations in *GNA11* in the germline leading to altered sensitivity of cells to extra-cellular calcium concentrations have been described in autosomal dominant hypoparathyroidism and hypocalculric hypercalcaemia respectively (28). One of these mutations (*GNA11*^{R60L}) has been characterised as less activating than *GNA11*^{Q209L} (25). This pattern of less severe mutations being supportable in the germline, whereas more severe mutations can survive only by mosaicism, once again confirms Happle's established theory (23). Patients with PPV and Sturge-Weber syndrome have not been documented to have abnormalities of calcium homeostasis, however intravascular calcification can be a feature of neurological abnormalities in PPV, which could hypothetically involve localized mosaic calcium imbalances. This is an area that merits future careful research.

A causal link between our genetic findings and mechanism is strongly supported by the mosaic zebrafish models demonstrated here, where expression of *GNA11*^{R183C} or *GNA11*^{Q209L} leads to ectopic and increased numbers of melanocytes in the epidermal and dermal layers, recapitulating the human phenotype of dermal melanocytosis. Over-expression of wild-type *GNA11* in melanocytes also leads to a low level of pigmentary mosaicism in zebrafish, underscoring the importance of close regulation of G-protein coupled receptor signaling in the melanocyte lineage. No other mosaic animal models of *GNA11* gain-of-function mutations exist, however further conformation of our findings comes from germline hypermorphic alleles of *GNA11* which lead to increased cutaneous pigmentation in the murine *Dsk* phenotype (29).

We have found no evidence for the now-retracted theory of twin-spotting or didymosis. Rather we have shown that a single somatic mutation in *GNA11* or *GNAQ* is responsible for

both types of cutaneous lesion in PPV, mirroring closely the pathogenesis of the disparate birthmarks seen in *HRAS* mosaicism (30). We propose that extensive dermal melanocytosis and PPV are members of an expanding group of heterotrimeric G-protein alpha subunit gene mosaic conditions, joining McCune-Albright syndrome (31), caused by mosaicism for gain-of-function mutations in *GNAS*, and Sturge-Weber syndrome, caused by mosaic gain-of-function mutations in *GNAQ* (23). We also propose that *GNAQ* mosaicism forms a spectrum from Sturge-Weber syndrome, through PPV, to extensive dermal melanocytosis. This knowledge will allow accurate clinical molecular diagnosis of a subset of extensive dermal melanocytosis and of PPV, leading to identification of neonates at risk of serious complications associated with these birthmarks. Importantly, it will also pave the way for therapeutic options in these children.

Materials and Methods

All human and animal studies were approved by the authors' research ethics review boards. Declaration of Helsinki protocols were followed, and all patients gave written informed consent. Eleven patients from four international centres were recruited with written consent for genetic research, approved by the local Research Ethics Committees. Patients were classified by clinical phenotype, three having extensive or atypical dermal melanocytosis, and eight having PPV, with representatives of subtypes I, II (cesioflammea), III (spilorosea), V (cesiomarmorata) (supplementary table 1, Fig. 1), and also the unclassifiable achromico-melano-marmorata type (32). Blood samples and skin biopsies were taken from each patient, and in those with PPV skin was biopsied from both the vascular and pigmentary birthmarks where possible.

Selective Amplification of Mutant Alleles of candidate genes GNA11 and GNAQ for Sanger sequencing

DNA was extracted from whole blood and directly from fresh skin lesion samples using the DNeasy Blood and Tissue Kit (Qiagen) and from paraffin embedded tissue using the RecoverAll total nucleic acid extraction kit for FFPE (Life Technologies). To maximize detection of mutant alleles at low percentage mosaicism we designed restriction enzyme digests of the normal allele at hotspots codons 183 and 209 of *GNA11* and 183 of *GNAQ* using validated methods (33) and Sanger sequencing. Primer sequences and restriction enzymes for each hotspot are shown in supplementary table 2. Touchdown PCR programmes were used throughout, with 35 cycles for the first PCR, and 25 for the second.

Targeted deep sequencing of GNA11 and GNAQ and data analysis

We performed targeted deep sequencing of the regions spanning mutations previously identified by selective amplification of mutant alleles in all samples where DNA quality was sufficient (as determined by the presence of a band above 10 kb size on agarose gel). In subjects with no identified mutation, all coding regions of *GNAQ* and *GNA11* were screened using the same method. Targeted regions were amplified using custom intronic primers and standard long-range PCR protocols. PCR products were purified and libraries were prepared using the Nextera XT DNA Sample Preparation kit (Illumina). Samples were then pooled and sequenced on a MiSeq instrument (Illumina) according to the manufacturer's recommendations for paired-end 150-bp reads. In-depth sequencing was performed to achieve a sequencing depth of at least 1,000 reads for all targeted coding bases and splice junctions. Identification of candidate variants was performed as described previously(34). Briefly, all targeted bases were systematically screened to count all sites with at least one read not matching the reference sequence, using a base-quality threshold of 30. Candidate post-zygotic variants were confirmed by at least one independent experiment in all DNA samples available from the patient.

Zebrafish model

To test the causality and model the effects of the mutation, we injected zebrafish embryos with wild-type human *GNA11*, $GNA11^{R183C}$ or $GNA11^{Q209L}$ expressed from the melanocyte *mitfa* promoter, and grew the genetically mosaic animals to adulthood. All zebrafish work was done in accordance with United Kingdom Home Office Animals (Scientific Procedures) Act (1986) and approved by the University of Edinburgh Ethical Review Committee.

The human *GNA11* cDNA clone was purchased from Origene, UK (purchased from NM_002067.1 precloned into an untagged pCMV6-XL4 vector, cat. number SC303115). Mutant GNA11Q209L(626a> t) was generated by site-directed genesis PCR with primers (forward: 5'- GATGTGGGGGGCCTGCGGTCGGAGCGGAGG -3', reverse: 5'-CCTCCGCTCCGACCGCAGGCCCCCCACATC-3'). Mutant GNA11R183C (547c>t) was also generated with primers (forward: 5'-CGTGCTGCGGGTCTGCGTGCCCACCACCG-3', reverse: 5'-CGGTGGTGGGCACGCAGACCCGCAGCACG-3'). The wildtype and mutant GNA11 cDNAs were cloned together with the zebrafish *mitfa* gene promoter into the pDestTol2CG2 expression vector using the Tol2kit gateway cloning method(35), resulting *mitfa*-GNA11, *mitfa*-GNA11Q^{209L} and *mitfa*-GNA11R^{183C} constructs. For selection purposes, these constructs contain an additional GFP gene expressed from the heart *cml* promoter. Two nl of mixed mitfa-GNA11 plasmid DNA and Tol2 mRNA (62.5ng/µl and 70ng/µl respectively) was injected into 1-cell stage zebrafish embryos. Zebrafish embryos with GFP transgenic marker in the heart were selected and grown to adulthood.

Adult zebrafish were anesthetized in 50mg/L tricaine solution and 1x images from both sides of the fish were taken under a stereomicroscope. Dark patches of melanocyte lesions with area larger than that of one scale were counted. Adult zebrafish were sacrificed by immersion in tricaine solution as directed by Home Office Schedule 1 methods. Zebrafish were then dissected in half transversely to increase penetration of the fixative, and fixed in 4% freshly prepared paraformaldehyde (Electron Microscopy Sciences, USA) at 4ºC for 3 days. Samples were then washed in PBS, and decalcified in 0.5M EDTA pH8 for 5 days before storage in 70% ethanol. Samples were embedded in paraffin wax and sectioned at 5µm thickness. For Haematoxylin and Eosin (H&E) staining slides were deparaffinised in xylene twice for 5 min, and then were rehydrated through graded alcohol solutions (100%,

90%, 70%, 50% and 30%; 3 min each) and stopped in water. Slides were stained with Mayer's Hematoxylin and Eosin following the standard H&E staining procedure.

Analysis of downstream effectors of GNA11in human cell line in culture

To characterize the functional effect of mutations on downstream signaling pathways HEK293T cells were transfected with vector, wild type *GNA11* or mutant *GNA11* constructs encoding R183C and Q209L. Q209L was used as a positive comparator as it is a more studied mutation in *GNA11*. Flag-tagged GNA11 WT, R183C and Q209L constructs and vector alone control (pDEST26, Invitrogen) were transfected into HEK293 cells using lipofectamine 2000 (Invitrogen), according to manufacturer's instructions. Cells were cultured for a further 24 hours and protein lysates were prepared by boiling in a denaturing SDS buffer (2% 2-mercaptoethanol, 2% SDS, 10mM Tris pH 7.5) for 10 minutes. Levels of GNA11 effector activation were assessed by western blot with the following antibodies at the following concentrations: Rabbit anti pSerine473 Akt (Cell Signalling Technologies, 1/500), Rabbit anti-Total Akt (1/1000, Cell signalling technologies) , Rabbit anti-phospho T180/Y182 p38 MAPK (1/500, Cell Signalling technologies), Rabbit anti-Total p38 MAPK (1/500, Cell signaling technologies), Mouse anti-phospho T183/Y185 SAPK/JNK (1/500, Cell signaling technologies), Rabbit anti-total SAPK/JNK (1/500, Cell Signalling Technologies), pT202/Y204 ERK (Cell Signalling technologies 1/500) and Rabbit anti-Total ERK 1,2 (1/1000, Cell Signalling technologies), Mouse anti-Flag (DYKDDDDK tag) (1/500, Cell Signalling technologies), Rabbit anti-GNA11 (Genetax, 1/500), and Mouse anti GAPDH (1/2000, Millipore).

Primary antibody incubations were in TBST (100mM Tris HCl, 0.2M NaCl, 0.1% Tween-20 (v/v) containing 5% bovine serum albumin (Sigma, Gillingham, UK) or 5% skimmed

milk powder either overnight at 4^{o}C or for 1-2 h at room temperature, while secondary antibody incubations were in 5% skimmed milk powder for 1 h at room temperature. The following concentrations were used; swine anti rabbit-HRP (DakoCytomation) 1:3000; rabbit anti mouse HRP (DakoCytomation) 1:2000. Protein was visualized using luminol reagent (Santa Cruz Biotechnologies). Densitometry of bands was performed using thresholded images in the ImageJ suite (http://imagej.nih.gov/ij/)

Conflict of Interest

The authors state no conflicts of interest.

Acknowledgements

We wish to thank the subjects and families involved in the study.

V.K. and laboratory research in London was funded by the Wellcome Trust, award number WT104076MA, and by the National Institute for Health Research Biomedical Research Centre at Great Ormond Street Hospital for Children NHS Foundation Trust and University College London. R.O'S. is funded by the Livingstone Skin Research Centre, UCL Institute of Child Health, London.

E.E.P. and Z.Z. are funded by the Medical Research Council, Human Genetics Unit, UK.

Laboratory work in Dijon was funded by the Agence Nationale de la Recherche (ANR-13-PDOC-0029 to J.-B.R), the Groupe Interrégional de Recherche Clinique et d'Innovation (GIRCI) Est (to J.-B.R), and the Programme Hospitalier de Recherche Clinique (PHRC) National (to P.V.).

References

1. Cordova A. The Mongolian spot: a study of ethnic differences and a literature review. Clin Pediatr (Phila). 1981;20(11):714-9.
2. Gupta D, Thappa DM. Mongolian spots--a prospective study. Pediatr Dermatol. 2013;30(6):683-8.
3. Igawa HH, Ohura T, Sugihara T, Ishikawa T, Kumakiri M. Cleft lip mongolian spot: mongolian spot associated with cleft lip. J Am Acad Dermatol. 1994;30(4):566-9.
4. Teekhasaenee C, Ritch R, Rutnin U, Leelawongs N. Ocular findings in oculodermal melanocytosis. Arch Ophthalmol. 1990;108(8):1114-20.
5. Shields CL, Kaliki S, Livesey M, Walker B, Garoon R, Bucci M, et al. Association of ocular and oculodermal melanocytosis with the rate of uveal melanoma metastasis: analysis of 7872 consecutive eyes. JAMA Ophthalmol. 2013;131(8):993-1003.
6. Hanson M, Lupski JR, Hicks J, Metry D. Association of dermal melanocytosis with lysosomal storage disease: clinical features and hypotheses regarding pathogenesis. Arch Dermatol. 2003;139(7):916-20.
7. Ota M, Kawamura T, Ito N. . Phakomatosis pigmentovascularis. Japanese Journal of Dermatology. 1947; 52:1-31.
8. Hasegawa Y, Yasuhara, M. A variant of phakomatosis pigmentovascularis. Skin Research. 1979;21:178-86.
9. Happle R. Phacomatosis pigmentovascularis revisited and reclassified. Arch Dermatol. 2005;141(3):385-8.
10. Danarti R, Happle R. Paradominant inheritance of twin spotting: phacomatosis pigmentovascularis as a further possible example. Eur J Dermatol. 2003;13(6):612.
11. Happle R. Mosaicism in human skin Springer-Verlag; 2013.
12. Shields CL, Kligman BE, Suriano M, Viloria V, Iturralde JC, Shields MV, et al. Phacomatosis pigmentovascularis of cesioflammea type in 7 patients: combination of ocular pigmentation (melanocytosis or melanosis) and nevus flammeus with risk for melanoma. Arch Ophthalmol. 2011;129(6):746-50.
13. Teekhasaenee C, Ritch R. Glaucoma in phakomatosis pigmentovascularis. Ophthalmology. 1997;104(1):150-7.
14. Henry CR, Hodapp E, Hess DJ, Blieden LS, Berrocal AM. Fluorescein angiography findings in phacomatosis pigmentovascularis. Ophthalmic Surg Lasers Imaging Retina. 2013;44(2):201-3.
15. Vidaurri-de la CH, Tamayo-Sanchez L, Duran-Mckinster C, Orozco-Covarrubias ML, Ruiz-Maldonado R. Phakomatosis pigmentovascularis II A and II B: clinical findings in 24 patients. JDermatol. 2003;30(5):381-8.
16. Hall BD, Cadle RG, Morrill-Cornelius SM, Bay CA. Phakomatosis pigmentovascularis: Implications for severity with special reference to Mongolian spots associated with Sturge-Weber and Klippel-Trenaunay syndromes. Am J Med Genet A. 2007;143A(24):3047-53.
17. Tsuruta D, Fukai K, Seto M, Fujitani K, Shindo K, Hamada T, et al. Phakomatosis pigmentovascularis type IIIb associated with moyamoya disease. Pediatr Dermatol. 1999;16(1):35-8.
18. Vidaurri-de la Cruz H, Tamayo-Sanchez L, Duran-McKinster C, Orozco-Covarrubias Mde L, Ruiz-Maldonado R. Phakomatosis pigmentovascularis II A and II B: clinical findings in 24 patients. J Dermatol. 2003;30(5):381-8.

19. Chhajed M, Pandit S, Dhawan N, Jain A. Klippel-Trenaunay and Sturge-Weber overlap syndrome with phakomatosis pigmentovascularis. Journal of pediatric neurosciences. 2010;5(2):138-40.
20. Jeon SY, Ha SM, Ko DY, Hong JW, Song KH, Kim KH. Phakomatosis pigmentovascularis Ib with left-sided hemihypertrophy, interdigital gaps and scoliosis: a unique case of phakomatosis pigmentovascularis. J Dermatol. 2013;40(1):78-9.
21. Krema H, Simpson R, McGowan H. Choroidal melanoma in phacomatosis pigmentovascularis cesioflammea. Can J Ophthalmol. 2013;48(3):e41-2.
22. Tran HV, Zografos L. Primary choroidal melanoma in phakomatosis pigmentovascularis IIa. Ophthalmology. 2005;112(7):1232-5.
23. Shirley MD, Tang H, Gallione CJ, Baugher JD, Frelin LP, Cohen B, et al. Sturge-Weber syndrome and port-wine stains caused by somatic mutation in GNAQ. N Engl J Med. 2013;368(21):1971-9.
24. 2015 [cited 20th August 2015]. Available from: http://exac.broadinstitute.org.
25. Li D, Opas EE, Tuluc F, Metzger DL, Hou C, Hakonarson H, et al. Autosomal dominant hypoparathyroidism caused by germline mutation in GNA11: phenotypic and molecular characterization. The Journal of clinical endocrinology and metabolism. 2014;99(9):E1774-83.
26. Van Raamsdonk CD, Griewank KG, Crosby MB, Garrido MC, Vemula S, Wiesner T, et al. Mutations in GNA11 in uveal melanoma. N Engl J Med. 2010;363(23):2191-9.
27. Van Raamsdonk CD, Bezrookove V, Green G, Bauer J, Gaugler L, O'Brien JM, et al. Frequent somatic mutations of GNAQ in uveal melanoma and blue naevi. Nature. 2009;457(7229):599-602.
28. Nesbit MA, Hannan FM, Howles SA, Babinsky VN, Head RA, Cranston T, et al. Mutations affecting G-protein subunit alpha11 in hypercalcemia and hypocalcemia. N Engl J Med. 2013;368(26):2476-86.
29. Van Raamsdonk CD, Fitch KR, Fuchs H, de Angelis MH, Barsh GS. Effects of G-protein mutations on skin color. Nat Genet. 2004;36(9):961-8.
30. Groesser L, Herschberger E, Sagrera A, Shwayder T, Flux K, Ehmann L, et al. Phacomatosis pigmentokeratotica is caused by a postzygotic HRAS mutation in a multipotent progenitor cell. The Journal of investigative dermatology. 2013;133(8):1998-2003.
31. Weinstein LS, Shenker A, Gejman PV, Merino MJ, Friedman E, Spiegel AM. Activating mutations of the stimulatory G protein in the McCune-Albright syndrome. N Engl J Med. 1991;325(24):1688-95.
32. Boente Mdel C, Obeid R, Asial RA, Bibas-Bonet H, Coronel AM, Happle R. Cutis tricolor coexistent with cutis marmorata telangiectatica congenita: "phacomatosis achromico-melano-marmorata". Eur J Dermatol. 2008;18(4):394-6.
33. Kinsler VA, Thomas AC, Ishida M, Bulstrode NW, Loughlin S, Hing S, et al. Multiple congenital melanocytic nevi and neurocutaneous melanosis are caused by postzygotic mutations in codon 61 of NRAS. J Invest Dermatol. 2013;133(9):2229-36.
34. Riviere JB, Mirzaa GM, O'Roak BJ, Beddaoui M, Alcantara D, Conway RL, et al. De novo germline and postzygotic mutations in AKT3, PIK3R2 and PIK3CA cause a spectrum of related megalencephaly syndromes. Nat Genet. 2012;44(8):934-40.
35. Kwan KM, Fujimoto E, Grabher C, Mangum BD, Hardy ME, Campbell DS, et al. The Tol2kit: a multisite gateway-based construction kit for Tol2 transposon transgenesis constructs. Dev Dyn. 2007;236(11):3088-99.

Competing financial interests

The authors declare no competing financial interests.

Table 1

Clinical phenotype and *GNA11 and GNAQ* genotypes with percentage mosaicism (where available) of different samples from eight patients with PPV (patients 1-8), and three patients with extensive dermal melanocytosis with no vascular phenotype (patients 9-11), showing post-zygotic mosaicism. For coordinates and exact wild-type and mutant allele numbers please see supplementary table 3. Where mutant allele detection is less than 1% we cannot confidently distinguish this from background noise despite the depth of coverage, and therefore these samples are assigned as wildtype. WT = wild-type; N/A = not applicable.

Patient	Diagnosis	Pigmentary skin lesion	Vascular skin lesion	Blood	Other samples	Result
1	PPV unclassifiable (I) type, capillary malformation on face (including forehead) and trunk, pigmentary lesions on limbs and trunk, linear sebaceous naevus on scalp, linear woolly hair; glaucoma; no overgrowth or neurological abnormalities		*GNA11* p.R183C 5.3%	WT 0.0%		*GNA11* p.R183C mosaic
2	PPV cesioflammea (II) type, capillary malformation on face (including forehead), scleral melanocytosis (no dermal melanocytosis); no overgrowth, ophthalmological or neurological abnormalities		*GNA11* p. R183S (novel)		Buccal swab *GNA11* p.R183S 7.9%; Normal skin WT	*GNA11* p.R183S mosaic
3	PPV cesioflammea (II) type, capillary malformation on face (including forehead), trunk, limbs; naevus anaemicus; dermal melanocytosis on trunk, scleral melanocytosis; bilateral glaucoma; renal vascular hypertension;		*GNAQ* p.R183Q 6.4%	WT 0.0%	Pigmented ocular tissue *GNAQ* p.R183Q	*GNAQ* p.R183Q mosaic

	hemihypertrophy; macrocephaly; CNS MRI - enlarged supratentorial subarachnoid space, enlarged lateral ventricles, increased arachnoid vascular network, asymmetrical venous flow, absence of pial angioma				11.0%	
4	PPV cesioflammea (II) type, capillary malformation face (including forehead), trunk, limb; dermal melanocytosis trunk and limb; growth delay, small teeth, developmental delay; no overgrowth, ophthalmological or radiological neurological abnormalities		*GNAQ* p.R183Q 5.0%	WT 0.0%		*GNAQ* p.R183Q mosaic
5	PPV cesioflammea (II) type, capillary malformation on face (including forehead), trunk, foot, dermal melanocytosis on face (including forehead), trunk, limbs; seizures, moderate global developmental delay, overgrowth, bilateral glaucoma, SWS-like pial angioma on MRI CNS	WT 0.0%	WT 0.0%	WT 0.0%		Wild type
6	PPV achromico-melano-marmorata type (unclassifiable in both classifications), pigmentary and vascular lesions affecting trunk and limbs; undergrowth of one leg (both affected by vascular lesions), no ophthalmological or neurological abnormalities		*GNA11* p.R183C	WT		*GNA11* p.R183C mosaic
7	PPV spilo-rosea type (III), pigmentary and vascular lesions affecting trunk and limbs, not face; no overgrowth, ophthalmological or neurological abnormalities	WT 0.0%	WT 0.0%	WT 0.0%		WT
8	PPV cesiomarmorata type (V), pigmentary lesions on trunk, vascular lesions on face (including forehead), trunk, limbs; mild developmental delay however MRI CNS showed periventricular leukomalacia consistent with premature delivery; no overgrowth, or ophthalmological abnormalities	*GNA11* p.R183C 15.5%	*GNA11* p.R183C 9.6%	WT 0.3% same mutation		*GNA11* p.R183C mosaic
9	Extensive and multiple dermal melanocytosis affecting trunk	*GNAQ*	N/A	WT		*GNAQ*

	and limbs; no overgrowth, ophthalmological or neurological abnormalities	p.R183Q 2%		0.1% same mutation		p.R183Q mosaic
10	One large (>20cm) dark, well-defined and persistant R flank dermal melanocytosis; no overgrowth, ophthalmological or neurological abnormalities	*GNAQ* p.Q209P 5.7%	N/A	WT 0.1% same mutation		*GNAQ* p.Q209P mosaic
11	Extensive and multiple dermal melanocytosis affecting trunk; no overgrowth, ophthalmological or neurological abnormalities	WT 0.0%	N/A	WT 0.0%		WT

Figure legends

Figure 1

Clinical examples of dermatological, ophthalmological and neurological aspects of PPV. Written consent for publication was obtained in all cases.

a-c) dermal melanocytosis and capillary malformation (port wine stain type) on the face, extensive dermal melanocytosis on the back and legs, capillary malformation on the sole of the right foot;

d) bilateral scleral melanocytosis with bilateral glaucoma, with capillary malformation and hemihypertrophy just visible on right face;

e) axial T1-weighed MR image of the brain the level of the lateral ventricles, after administration of intravenous Gadolinium contrast agent, showing bilateral and asymmetrical thickening and enhancement of the pia mater.

Figure 2

Sequencing results demonstrating mosaic *GNA11* and *GNAQ* mutations

a) Sanger sequencing of skin biopsy showing a very low peak in *GNA11* at position c.547C>T (p.Arg183Cys) (asterisk)

b) Sanger sequencing of the same skin biopsy DNA after restriction enzyme digest of the normal allele, and hemi-nested amplification, revealing the mutation (asterisk)

c) Targeted next generation sequencing showing low allele percentage mutations in skin but undetectable in blood, *GNA11* c.547C>T (p.Arg183Cys) in 5% of reads

d) *GNAQ* c.548G>A (p.Arg183Gln) in 6% of reads from skin but undetectable in blood

Figure 3

Mutant *GNA11* leads to activation of downstream signaling pathways

a) Western blot for Flag, Total GNA11 and the phosphorylated and total p38, JNK, ERK and AKT in total protein lysates from HEK293T cells transfected with either vector, wildtype *GNA11* (WT) or one of two mutants R183C or Q209L mutant *GNA11*.

b) Graph shows the ratio of phosphorylated to total p38, JNK, ERK and AKT normalized by the actin loading control. Bars indicate one standard deviation.

Figure 4

Mosaic expression of *GNA11* promotes ectopic pigmentary lesions in zebrafish.

a) Images of adult zebrafish mosaic for *GNA11*, $GNA11^{R183C}$ *or* $GNA11^{Q209L}$ expression. Large, ectopic pigmentary lesions are indicated next to white arrows. Dashed box indicates zoomed areas that show detail of pigmentary lesions

b) Numbers of pigmentary lesions per fish expressing *GNA11*, $GNA11^{R183C}$ or $GNA11^{Q209L}$. Dark circles indicate ectopic pigmentary lesions; white circles indicate fish without pigmentary lesions.

c) Histology H&E staining of a wild type and $GNA11^{R183C}$ zebrafish skin at 100x and 400x magnification. Melanocytes are clearly visible in the dermis by the

black melanin (blue arrows), frequently also in the epidermis (not shown) and in a few cases within underlying muscle (yellow arrow).

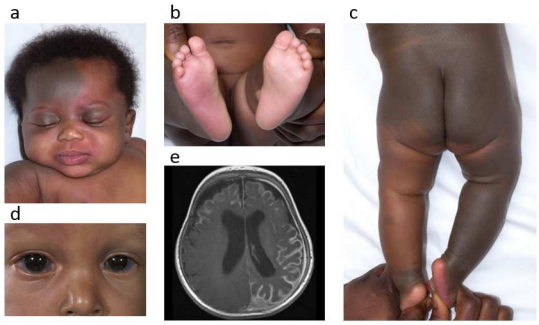

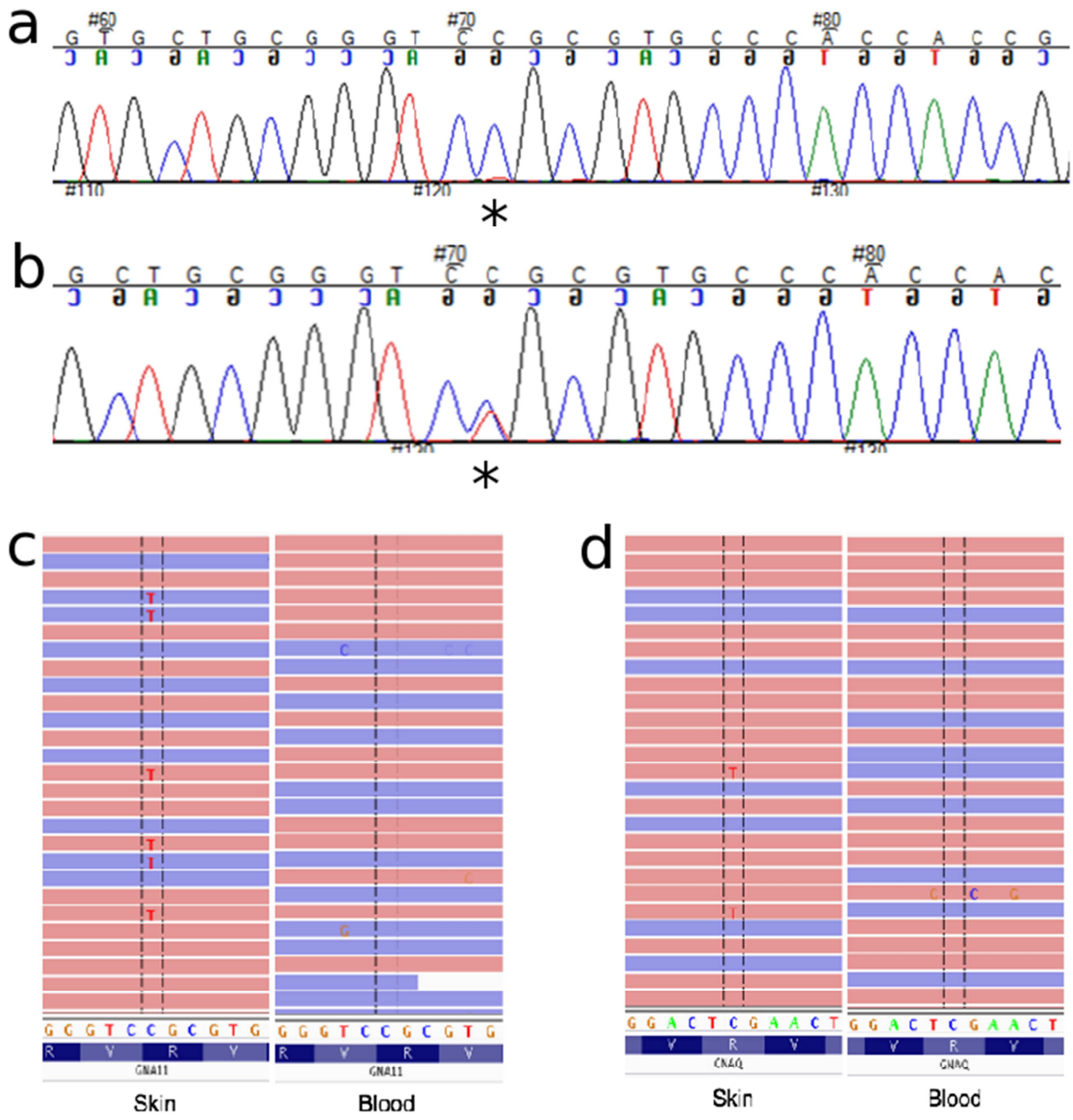
a
b
c
d
Skin
Blood
Skin
Blood

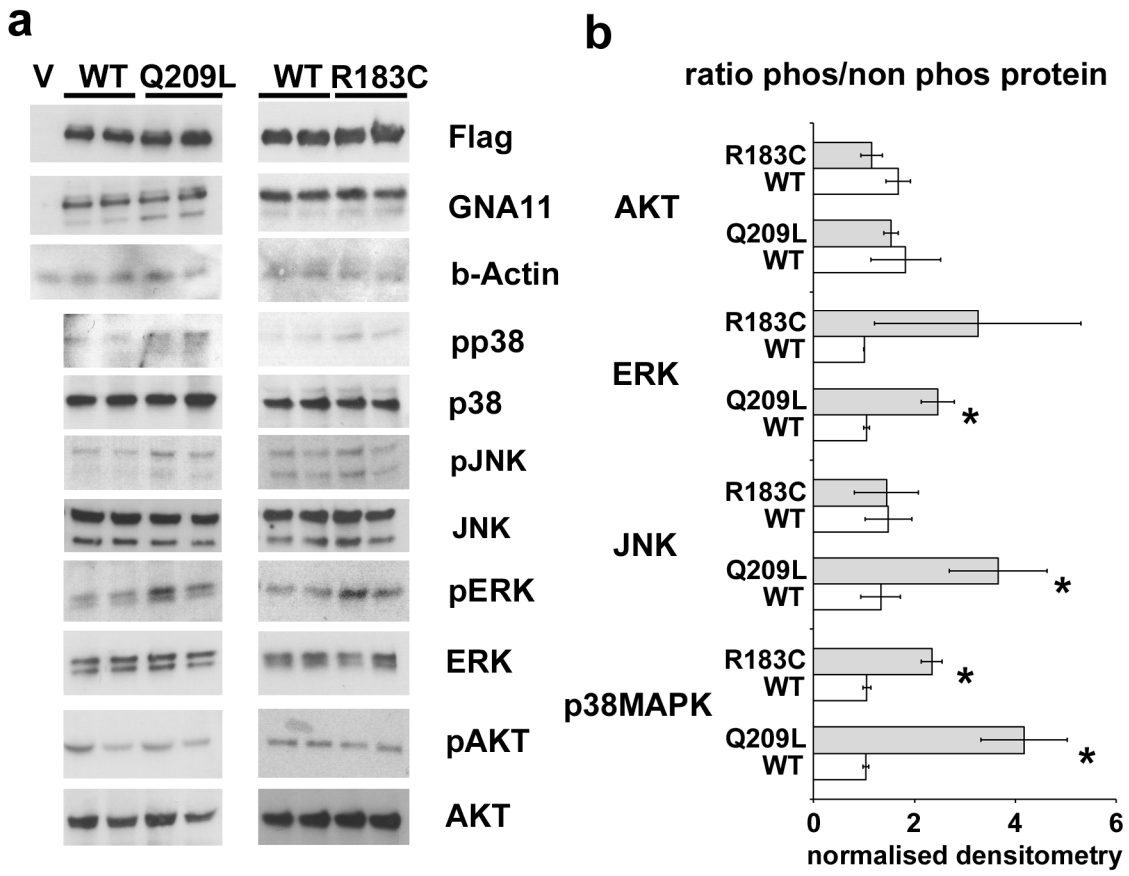

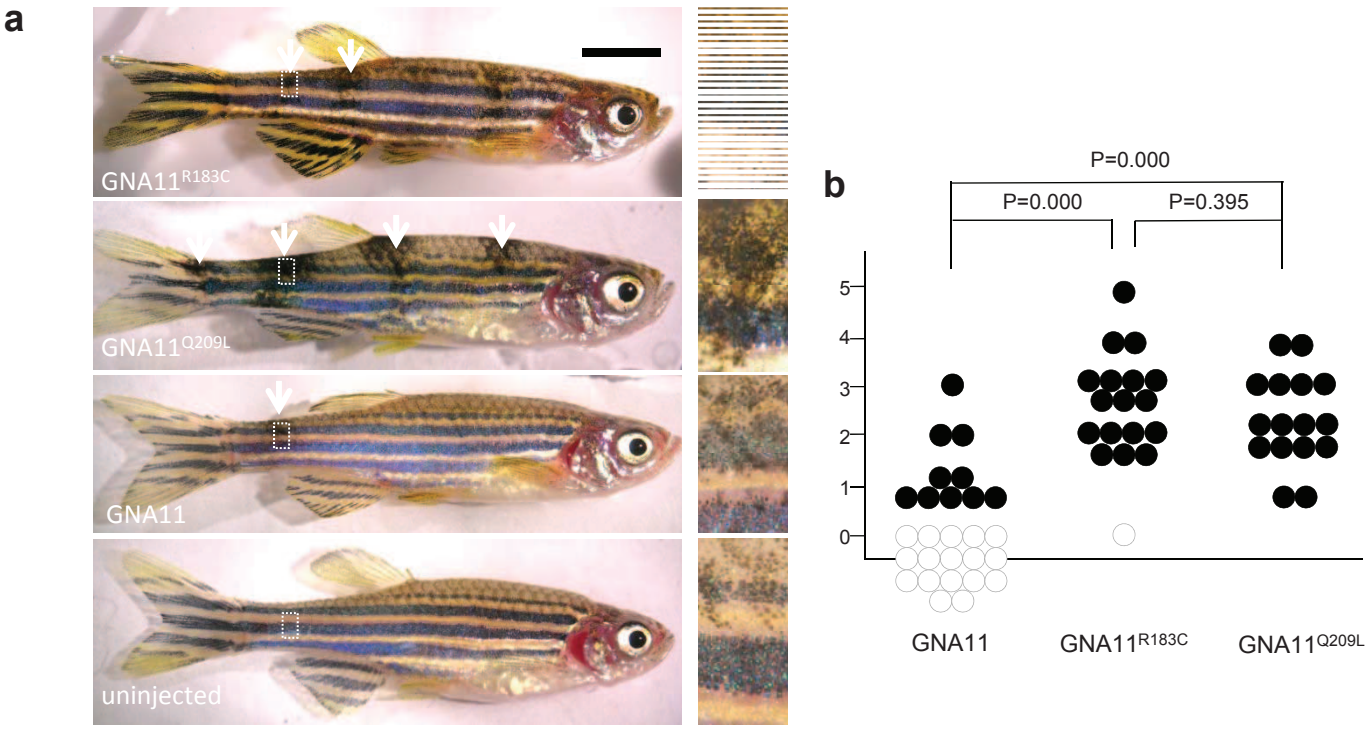
a
GNA11R183C
GNA11Q209L
GNA11
uninjected
b
P=0.000
P=0.000
P=0.395
5
4
3
2
1
0
GNA11
GNA11R183C
GNA11Q209L

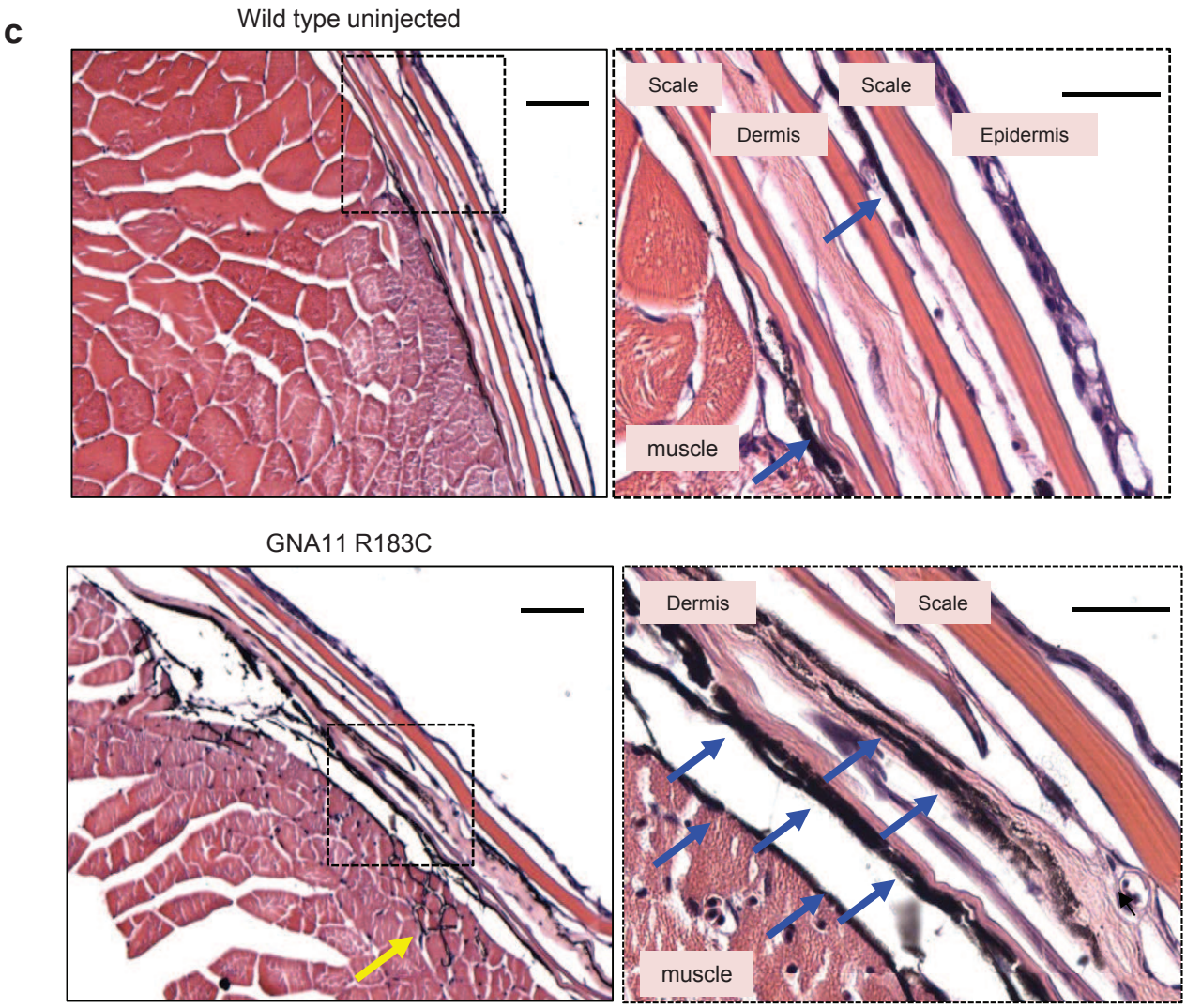
c
Wild type uninjected
Scale
Scale
Dermis
Epidermis
muscle
GNA11 R183C
Dermis
Scale
muscle